Nuclear Instruments and Methods in Physics Research A257 (1987) 233–243
North-Holland, Amsterdam

DETERMINATION OF THE SPIN ALIGNMENT IN HEAVY-ION REACTIONS WITH THE SPIN SPECTROMETER

K.J. HONKANEN *, F.A. DILMANIAN ** and D.G. SARANTITES

Department of Chemistry, Washington University St. Louis, MO 63130, USA

S.P. SORENSEN +

Oak Ridge National Laboratory Oak Ridge, TN 37831, USA

Received 11 February 1987

A detailed procedure is outlined that permits one to deduce the spin direction in heavy-ion fusion reactions on an event-by-event basis using data from the spin spectrometer at the Holifield Heavy Ion Research Facility of Oak Ridge National Laboratory. The parameters that govern the ability of the spin spectrometer in determining the spin direction, namely the γ-ray multiplicity, the multipolarity, the crystal-to-crystal scattering, and coincidence summing, are examined in detail. Removal of detectors from the complete spectrometer causes large misalignment in the deduced spin distributions. A procedure to correct for this induced misalignment based on local density distributions is presented. Some results from measurement of angular distributions of α-particles using the spin alignment method are also discussed.

1. Introduction

Angular distributions of γ rays or α particles emitted in heavy-ion fusion reactions provide valuable information about the structure of nuclei. The value of such information has been demonstrated in discrete γ ray spectroscopy or, at higher excitations, in continuum γ ray spectroscopy [1–3], as well as in studies on the shapes of highly excited and rapidly rotating nuclei from α particle angular correlations. [4] In the past, the only way to obtain this information was measurement of angular distributions relative to the beam direction. Since the relevant correlation is between the direction of emission and that of the total angular momentum, one has to integrate over the possible spin directions about the beam. Besides that, there was little or no angular momentum selectivity in the reaction systems.

In recent years the availability of 4π γ ray multidetector arrays such as the spin spectrometer [5,6] at the Holifield Heavy Ion Research Facility makes it possible, through event-by-event measurement of the γ-ray multiplicity, to select a narrow range of spins in the evaporation residues in order to study a variety of nuclear properties by measurements of associated γ-rays or charged particles. Such measurements carried out with the spin spectrometer have provided, at least for good rotors, rather narrow selections of spin [6,7]. Furthermore, in angular distribution studies of γ rays or α particles, the use of the spin spectrometer allows us to dispense with the integration over the possible spin orientations and to measure the emission probability of γ rays or of α particles with respect to the spin direction of the residual nuclei. Since the directions of total angular momentum and the residual spin direction are highly correlated in high spin fusion reactions, one can simply study the emission of radiation with respect to the residual spin direction.

In this paper we describe in detail a method for deriving the spin direction on an event-by-event basis from spin spectrometer data. In sect. 2 we present the formalism on which the algorithm for the spin alignment method is based. The factors influencing the ability of the spin spectrometer to find the spin direction (i.e. the shape of the spin alignment response) are described in sect. 3. The results of calculations based on simulated events, including the effect of γ ray multipolarity and the presence of holes in the spectrometer on the response function are given in sect. 4. Finally, sect. 5 includes some examples of use of the spin alignment method in deriving the angular distribution of α particles emitted from high-spin and high-excitation states in nuclei.

* Present address: Department of Physics, University of Jyväskylä, Jyväskylä, Finland. (Deceased.)
** Present address: Medical Department, Brookhaven National Laboratory, Upton, NY 11973, USA.
+ Present address: Department of Physics and Astronomy, University of Tennessee, Knoxville, TN 37996, USA.

2. The spin alignment method

2.1. The γ radiation pattern

The angular distribution pattern for pure multipole radiation LM emitted with respect to the spin direction is given by [8]

$$Z_{LM}(\theta, \phi) = \frac{1}{2}\left[1 - \frac{M(M+1)}{L(L+1)}\right] |Y_{L,M+1}|^2 + \frac{1}{2}\left[1 - \frac{M(M-1)}{L(L+1)}\right] |Y_{L,M-1}|^2 + \frac{M^2}{L(L+1)} |Y_{LM}|^2. \quad (1)$$

For heavy nuclei produced in heavy-ion fusion reactions it is known that in the γ ray energy spectrum a so-called quadrupole bump is observed that consists primarily of quadrupole E2 stretched ($\Delta I = -2$) radiation. At higher energies, above the quadrupole bump, an incoherent admixture of stretched and unstretched dipole radiation is responsible for the essentially isotropic angular distributions observed [2,9]. This indicates that a good approximation would be to consider only stretched E2, ($\Delta I = -2$, $L = 2$, $M = 2$), stretched dipole ($\Delta I = -1$, $L = 1$, $M = 1$), and nonstretched dipole ($\Delta I = 0$, $L = 1$, $M = 0$) multipole radiation in eq. (1). For these cases eq. (1) reduces to

$$Z_{22}(\theta) = \tfrac{5}{4}(1 - \cos^4\theta), \quad (2a)$$

$$Z_{11}(\theta) = \tfrac{3}{4}(1 + \cos^2\theta), \quad (2b)$$

$$Z_{10}(\theta) = \tfrac{3}{2}(1 - \cos^2\theta). \quad (2c)$$

These functions are illustrated in polar coordinates in fig. 1. It is clearly seen that the functions $Z_{22}(\theta)$ and $Z_{10}(\theta)$ have the shapes of a "doughnut" the hole axis of which coincides with the spin axis. In contrast, the stretched dipole case $Z_{11}(\theta)$ exhibits the shape of a "peanut" with the long axis along the spin direction. For γ rays of a given multipolarity emitted in cascade, the hit-pattern of the detectors in the spin spectrometer reflects a distribution pattern given by $Z_{LM}(\theta, \phi)\mathrm{d}\Omega$, which can be used to find the spin direction in space within a certain accuracy depending on certain factors discussed below. Therefore, the spin alignment method is based on the presence of a nonisotropic γ ray angular distribution caused by the preponderance of γ transitions with a particularly nonisotropic angular distribution with respect to the spin direction. For example, preponderance of stretched quadrupole and/or nonstretched dipole ($\Delta I = 0$) over stretched dipole ($\Delta I = -1$) transitions provide a high anisotropy. It is then possible to derive an algorithm to find the spin direction in the residual nuclei from where the γ cascade starts. The two multipolarities mentioned above appear to be typical for the de-excitation of nuclei formed in fusion reactions. The presence of a small number of stretched dipole transitions has the effect of filling in the hole of the "doughnut", but the distribution pattern has the appearance of an ellipsoid of rotation with its minor axis along the spin direction.

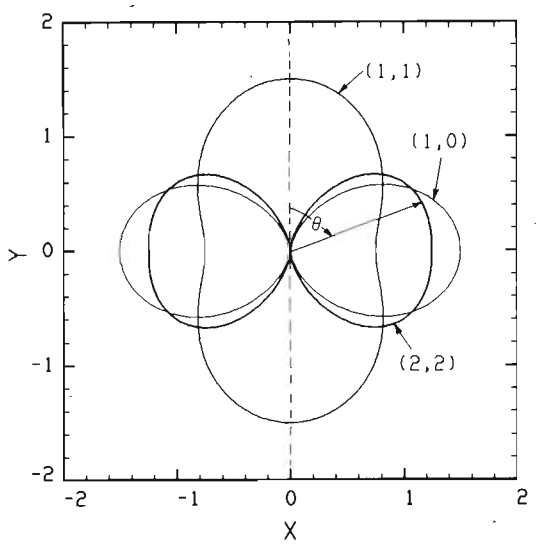

Fig. 1. Polar-coordinate plots of the angular distribution functions given in eqs. (2). The curves are labelled by the (L, M) values. The curve (2, 2) is for stretched quadrupole transitions, the curve (1, 1) is for stretched dipole ($\Delta I = -1$) and the (1, 0) curve is for nonstretched dipole transitions.

2.2. The spin alignment algorithm

In heavy ion fusion reactions at high spin values, the spin direction of both compound nucleus and evaporation residue lies in the plane perpendicular to the beam within a good approximation. The only disturbance comes from emission of light charged particles (p, d, t, α, and τ) and/or of neutrons, which broadens the spin alignment pattern to some extent, but leaves it on the average in the plane perpendicular to the beam direction. Thus a tight correlation between the residual and the initial spin direction is maintained.

For reactions other than fusion, for example in deeply inelastic collisions, the two residual nuclei can contribute to the γ cascades with the sum of their spins lying not necessarily in the plane perpendicular to the beam direction. In such a case, triaxial hit pattern describes the γ distribution pattern, with its shortest axis along the resultant spin direction. Because of this possibility, two algorithms are presented: a 3-dimensional one that accommodates the deviation from the plane perpendicular to the beam, and another 2-dimensional one for the case where the spin is confined to a plane.

The coordinate system is chosen with the z axis (x_3) along the beam direction and the x axis (x_1) in the vertical direction. Then the vector $\boldsymbol{x}_i = (x_{1i}, x_{2i}, x_{3i})$ points toward the ith detector in the spectrometer. If k detectors fire in an event, then the hit-pattern is defined by the covariance tensor:

$$\sigma_{ij} = \frac{k}{k-1}\left(\langle x_i x_j\rangle - \langle x_i\rangle\langle x_j\rangle\right), \tag{2}$$

where

$$\langle x_i\rangle = \frac{1}{k}\sum_{m=1}^{k} x_{im}, \quad \text{and} \quad \langle x_i x_j\rangle = \frac{1}{k}\sum_{m=1}^{k} x_{im}\cdot x_{jm}.$$

The eigenvalues λ_i and the eigenvectors $\boldsymbol{\epsilon}_i$ of the 3×3 matrix σ_{ij} specify the lengths and directions of the principal axes of the best-fit ellipsoid. More specifically, the lengths of the principal axes are given by $2\sqrt{\lambda_i}$ [10], and the direction of the spin coincides with the direction of the vector $\boldsymbol{\epsilon}_{\min}$ which corresponds to the smallest eigenvalue $\lambda_{\min}$. It can be shown [11] that the eigenvalues λ_n of the characteristic equation

$$\begin{vmatrix} \sigma_{11}-\lambda & \sigma_{12} & \sigma_{13} \\ \sigma_{12} & \sigma_{22}-\lambda & \sigma_{23} \\ \sigma_{13} & \sigma_{23} & \sigma_{33}-\lambda \end{vmatrix} = 0. \tag{3}$$

are given by

$$\lambda_n = -\frac{a_2}{3} + 2\,s\cos\frac{1}{3}\cos^{-1}\left(\frac{r}{s^3}\right) + (n-1)\frac{2\pi}{3}, \tag{4}$$

where $s = \frac{1}{3}(a_2^2 - 3a_1)^{1/2}$,

$r = (a_1 a_2 - 3a_0)/6 - a_2^3/27$

and $a_0 = \sigma_{11}\sigma_{23}^2 + \sigma_{22}\sigma_{13}^2 + \sigma_{33}\sigma_{12}^2 - \sigma_{11}\sigma_{22}\sigma_{33} - 2\sigma_{12}\sigma_{13}\sigma_{23}$

$a_1 = \sigma_{11}\sigma_{22} + \sigma_{11}\sigma_{33} + \sigma_{22}\sigma_{33} - \sigma_{12}^2 - \sigma_{13}^2 - \sigma_{23}^2$

$a_2 = -(\sigma_{11} + \sigma_{22} + \sigma_{33})$.

The polar and azimuthal angles (θ_n, ϕ_n) of the nth eigenvector are given by

$$\cos\theta_n = \left[1 + c_n^2 + (\lambda_n - \sigma_{33} - \sigma_{23}\sigma_n)^2/\sigma_{13}^2\right]^{1/2}, \tag{5}$$

and

$$\tan\phi_n = c_n\sigma_{13}/(\lambda_n - \sigma_{33} - \sigma_{23}c_n), \tag{6}$$

where

$$c_n = \frac{(c_{11} - \lambda_n)(\sigma_3 - \lambda_n) - \sigma_{13}^2}{\sigma_{12}\sigma_{13} - \sigma_{23}(\sigma_{11} - \lambda_n)}. \tag{7}$$

Thus, the final expression for the eigenvectors $\boldsymbol{\epsilon}_n$ is

$$\boldsymbol{\epsilon}_n = (\sin\theta_n\cos\phi_n, \sin\theta_n\sin\theta_n, \cos\theta_n). \tag{8}$$

If the eigenvalues are arranged in descending order $\lambda_1 > \lambda_2 > \lambda_3$, then the estimated spin direction is defined by the angles (θ_3, ϕ_3). Let $\psi = \tan^{-1}(-\epsilon_{23}/\epsilon_{13})$, then the angles (θ_3, ϕ_3, ψ) are the Euler angles that rotate the initial coordinate system to the one with the z axis along the estimated spin direction (θ_3, ϕ_3) and the x axis along the longest principal axis.

If the residual spin is confined into the plane perpendicular to the beam direction then eq. (6) reduces to:

$$\begin{vmatrix} \sigma_{22}-\lambda & \sigma_{23} \\ \sigma_{23} & \sigma_{33}-\lambda \end{vmatrix} = 0, \tag{9}$$

with solutions:

$$\lambda_{\pm} = \tfrac{1}{2}(\sigma_{22} + \sigma_{33}) \pm \left[\tfrac{1}{4}(\sigma_{22} - \sigma_{33})^2 + \sigma_{23}^2\right]^{1/2}.$$

Now, the spin direction along the polar angle $\phi°$ corresponding to the smaller eigenvalue λ_- is

$$\phi° = \tan^{-1}\frac{2\sigma_{23}}{(\sigma_{22} - \sigma_{33}) - \left[(\sigma_{22} - \sigma_{33})^2 + 4\sigma_{23}^2\right]^{1/2}}. \tag{10}$$

A FORTRAN routine to compute (θ, ϕ) in eq. (8) runs on a VAX 11/780 computer at the rate of $(1.5 + 0.05k)$ ms/event, while a routine for $\phi°$ in eq. (10) requires $(0.05k)$ ms/event only.

An alternative method devised by Holm [12] for estimating the direction of the spin, which is equivalent to that of eqs. (9) and (10), is given below. The shape of the projection of the ellipsoid onto the x–y plane containing the spin (that is the plane perpendicular to the beam) would be an ellipse or a "peanut". Fig. 2 illustrates the projected hit-pattern on the x–y plane for an event with 18 detectors fired. The projected pattern has two symmetry axes of x' and y', the shorter of which, y', is the estimated spin direction. The angle β can be determined by minimizing the expression

$$R'_{yy} = \sum_i (y_i')^2 = \sum_i (y_i\cos\beta - x_i\sin\beta)^2. \tag{11}$$

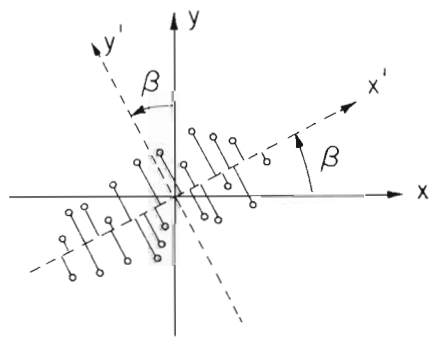

Fig. 2. Schematic representation of the scatter plot from the projection of an event of multiplicity 18 on the $x-y$ plane which is assumed to be perpendicular to the beam direction. The position of the y' axis which is obtained by minimizing the sum of the squares of the distances from the axis x' provides the estimated spin direction defined by the angle β.

By setting $(\partial R'_{yy}/\partial\beta) = 0$ we obtain:

$$\beta = \frac{1}{2}\tan^{-1}\left(\frac{2R_{xy}}{R_{xx} - R_{yy}}\right), \tag{12}$$

where:

$$R_{xx} = \sum_{i=1}^{k} x_i^2, \quad R_{yy} = \sum_{i=1}^{k} y_1^2, \quad \text{and} \quad R_{xy} = \sum_{i=1}^{k} x_i y_i, \tag{13}$$

with

$$x_i = r \sin\theta_i \cos\phi_i, \quad y_i = r \sin\theta_i \sin\phi_i, \quad \text{and}$$
$$z = r \cos\theta_i. \tag{14}$$

Here $\boldsymbol{r}_i = (x_i, y_i, z_i)$ is the vector pointing to the ith detector in the spectrometer. The computer algorithm for a rapid evaluation of β by using eq. (12) can be expedited by a priori evaluation of the quantities x_i^2, y_i^2, and $x_i y_i$ for each detector. For each event with different hit-pattern the appropriate sums in eqs. (13) are constructed and β is evaluated from eq. (12). This is a rapid procedure, with the rate of $\sim (0.03k)$ ms/event when implemented by a FORTRAN routine on the VAX 11/780 computer.

2.3. Correction algorithm for unequal detection efficiencies

The search procedures outlined above produce unbiased results as long as cylindrical symmetry is maintained in the spectrometer. The only detectors that may be removed from the spectrometer are the 0° and 180° detectors, and all the existing detectors should have equal efficiency for γ ray detection. This condition is hardly ever satisfied in realistic experimental situations. Asymmetries in the scattering chamber, and presence of internal triggering devices such as Si $(\Delta E, E)$ telescopes, the target holder and supporting rod, etc., result in variations as high as 35% in detection efficiencies of some detectors with respect to the average efficiency value. Furthermore, external detectors such as Ge detectors which require removal of one or more NaI detectors from the spectrometer introduce even larger perturbations. As it will be shown below, serious perturbations in the spin alignment response and the deduced distribution of the spin direction are caused by the above asymmetries.

A procedure has been developed to correct for the presence of holes or for unequal efficiencies in the spectrometer. For a particular hole or detector with hindered efficiency, it calculates the hit probability by using the local hit-patterns both around the detector site and around the inversion point in the opposite side of the spectrometer and casts a random number to decide if there is a hit or not. Considering the fact that γ emission is invariant under inversion up to a small relativistic shift of order $(v/c)^2$ in its angular distribution, this routine is quite adequate. The details of the hit-probability calculation follow.

Let Ω_i be the efficiency of detector i and $\langle\Omega\rangle$ the overall average efficiency. For a removed detector $\Omega_i = 0$, for a detector whose efficiency is hindered by absorption $\Omega_i/\langle\Omega\rangle < 1$, and for a detector whose efficiency is enhanced by scattering from nearby material $\Omega_i/\langle\Omega\rangle > 1$. A random-number based correction is applied to every detector with $\Omega_i/\langle\Omega\rangle \neq 1$.

We consider first the case $\Omega_i/\langle\Omega\rangle < 1$. Let the index j run over the 5 (or 6) closest detectors to the ith one and over the 6 (or 7) farthest ones for the pentagonal (hexagonal) ith detectors, respectively. We assign $P_j = 1$ or 0 if the jth detector did fire or not, respectively. If $P_i = 1$ no correction is required. If $P_i = 0$ then the local hit density ρ_i is

$$\rho_i = \frac{\sum P_j}{\sum \Omega_j} = \frac{\sum P_j}{N_i\langle\Omega\rangle}, \tag{15}$$

where the sum is over the index j and N_i is the number of detectors that are sampled including the ith one.

Since the lost efficiency is $(\langle\Omega\rangle - \Omega_i)$ then the probability that the ith detector would have fired if it had not been blocked is

$$q_i = \rho_i(\langle\Omega\rangle - \Omega_i) = \frac{\sum P_j}{N_i}\left(1 - \frac{\Omega_i}{\langle\Omega\rangle}\right). \tag{16}$$

Let η be a random number between 0 and 1. Then if $\eta \leq q_i$ we set P_i equal to 1, otherwise $P_i = 0$. For every detector with $P_i = 1$ the appropriate terms in eq. (13) are added.

Next we consider the case $\Omega_i/\langle\Omega\rangle > 1$. If $P_i = 0$ no correction is required. If $P_i = 1$ then the local density is again given by eq. (15). Now the gained efficiency is $(\Omega_i - \langle\Omega\rangle)$ and the probability that the ith detector overfired is

$$q_i = (\Omega_i - \langle\Omega\rangle)\rho_i = \left(\frac{\Omega_i}{\langle\Omega\rangle} - 1\right)\frac{\sum P_j}{N_i}. \tag{17}$$

Now, let η be a random number between 0 and 1. Then if $\eta \leq q_i$ we set P_i to 0, otherwise $P_i = 1$. Again, the outcome of the cast is introduced in the sums in eq. (13), i.e. the ith term is added if $P_i = 1$ and it is not if $P_i = 0$.

It should be emphasized that the accuracy of finding the spin direction, i.e. the width of the spin-detection response function, depends only on the γ ray angular distribution and not on the alignment of the nuclei in the measured ensemble. For example, for a spherical emission pattern a spherical hit pattern results and the spin alignment routine will produce an isotropic distribution of spins when it operates on events, even if the measured nuclei possess spin alignment. The factors controlling the distribution of hit patterns in the spin spectrometer are described in the following sections.

3. Simulation of events

In order to measure the response function of the spectrometer for determining the spin direction in residual nuclei, which represents the accuracy of the measurement, simulated events should be created by a routine that includes in detail all the factors involved in γ-ray emission and in γ-ray detection.

A Monte Carlo procedure has been devised to produce events of a given multiplicity, multipolarity (or an incoherent mixture of multipolarities) and γ ray energy. In this procedure M_γ photons are emitted in a spatial distribution dictated by the chosen composition of multipolarities. The detector efficiency and crystal-to-crystal scattering are derived, for the chosen γ ray energy, by the procedures described in ref. [6]. In this procedure we use the equal energy approximation [6] by assuming that all the energies in the cascade are equal to the average energy value in the cascades of interest. For individual NaI detectors the coincidence summing and the crystal-to-crystal scattering up to the third order are properly taken into account. The computer routine takes the efficiency values Ω_i for the 72 NaI detectors from a look-up table stored as a file. In this way, the efficiency of any detector can be changed by modifying this file. A detector is removed by setting $\Omega_i = 0$. It can also be assigned to have absorption ($\Omega_i < \langle\Omega\rangle$) or scattering ($\Omega_i > \langle\Omega\rangle$).

In this procedure a given number of events with a given single initial spin direction, or a specified distribution of spin directions, can be produced. In the following sections, for simplicity, we confine our discussion to the case that the spin is located in the plane perpendicular to the beam direction.

4. Spin alignment responses

4.1. Dependence of the response on multiplicity and multipolarity

The angular distribution of the hit-pattern, which is the response of the spin spectrometer to γ cascades, depends on the γ ray multiplicity M_γ, the γ ray energy and the multipolarity of the γ rays in the cascade. The importance of coincidence summing, which causes a reduction in the coincidence fold K (number of detectors firing), increases with M_γ and consequently its broadening effect on the spin alignment (SA) response also increases with M_γ. However, as M_γ increases the statistics within the event also increase and as a result the SA resolution improves. The extent of crystal-to-crystal scattering which also causes broadening of SA response is determined by E_γ and not by M_γ. The combined effect of these factors is seen in fig. 3. Here 10^5 events are created for each M_γ value consisting of

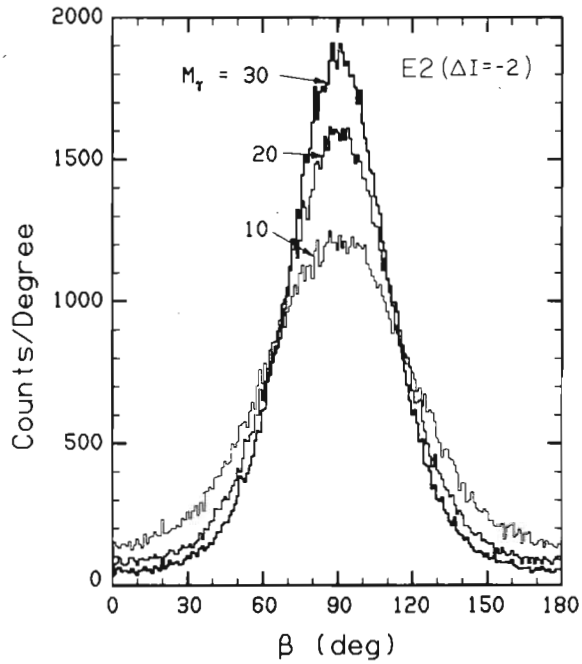

Fig. 3. Spin alignment resolution (SA response) of the spin spectrometer for cascades of M_γ 10, 20, and 30 γ rays, all stretched E2. Here 10^5 events were generated and sorted for each case. The original spin direction was at $\beta = 90°$. The resolution improves considerably with increasing M_γ.

stretched E2 transitions only. In all these simulations E_γ was taken to be 1 MeV. The events in each case were created with the spin orientation at 90° and the data were sorted with the SA search routine. The responses for $M_\gamma = 10$, 20, and 30 are shown in fig. 3. As expected, the responses peak at 90° and show that the resolution improves considerably with increasing γ ray multiplicity. These SA responses can be represented reasonably well by a Gaussian resting on a flat background. Fig. 4 shows the width of the Gaussian and the associated flat background as the fraction of the total number of events as a function of M_γ for cascades of stretched E2 transitions. It is seen that typical values for the fwhm vary between 45° and 65° as M_γ goes down from 35 to 10.

Since for most fusion reactions of interest the average γ ray energy is about 1.0–1.4 MeV, the average crystal-to-crystal scattering varies by very little from one reaction to the other. [6] Although this variation can be simulated by the equal-energy approximation, its effect on the SA response width is a minor one, and it is not included in the following discussion.

The variation of the SA resolution with γ ray multipolarity, however, is much more pronounced. This dependence will be demonstrated below in a series of selected examples. The examples include the effect of

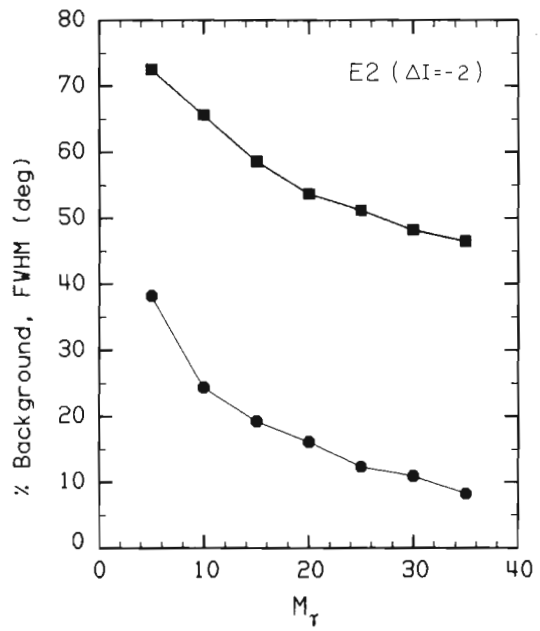

Fig. 4. Plots of the Gaussian width (solid squares) and the associated constant background as percentage of the total events (solid circles) obtained by fitting the SA responses as a function of M_γ for cascades of pure stretched E2 transitions. It is seen that both the full width at half maximum (fwhm) and flat background decrease as M_γ increases.

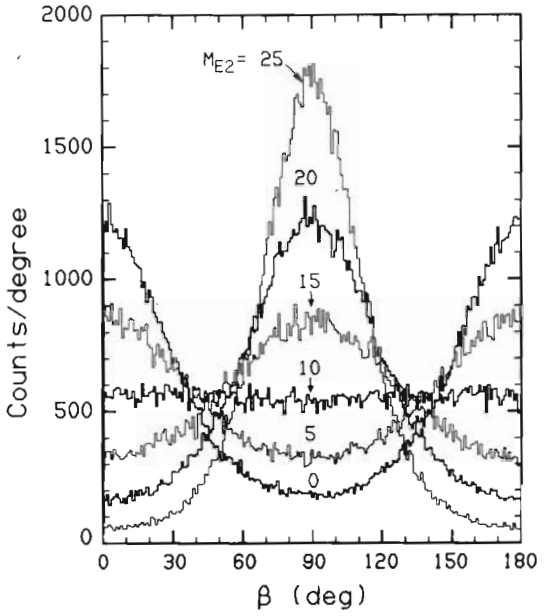

Fig. 5. Spin alignment responses for γ cascades with a constant value of total $M_\gamma = 25$, consisting of a sum of stretched dipole and stretched quadrupole transitions. The number of stretched E2 transitions is indicated in each case. It is seen that the SA resolution decreases as the number of stretched quadrupoles decreases (i.e. as the number of stretched dipoles increases). For $M_{E2} = 10$ and $M_{E1} = 15$ the SA response is completely flat and for $M_{E2} < 10$ and $M_{E1} > 15$ the peak value shifts by 90°.

admixing different numbers of stretched dipole transitions to stretched quadrupole transitions for a fixed value of total multiplicity M_γ'[$M_\gamma = M_{E2(\Delta I=-2)} + M_{E1(\Delta I=-1)}$]. Fig. 5 illustrates the results for the total multiplicity M_γ of 25 and for the $M_{E1(\Delta I=-2)}$ values varying from 0 to 25. It is clear from these results that the SA resolution decreases as the number of stretched E2 transitions decreases (i.e. as the number of dipoles increases). For $M_{E2} = 10$ and $M_{E1} = 15$ the SA response is flat. As the number of stretched E2 transitions is further decreased the peak of the SA response shifts by 90°, as expected (see fig. 1). Fig. 6 shows the variation of the widths of a fitted Gaussian and the fraction of constant background in the SA responses as a function of the number of stretched E2 transitions mixed with stretched E1 transitions for a fixed value of $M_\gamma = 25$. The data points illustrated are only those for which the E2 pattern dominates the shape of the hit-pattern.

It was pointed out earlier that the presence of nonstretched dipole transitions enhances the doughnutlike shape of the hit-pattern in a more pronounced way compared to the stretched E2 transitions. This effect is demonstrated in fig. 7, where the Gaussian widths and the background fractions for cascades of fixed total $M_\gamma = 25$ are plotted as a function of the number of stretched E2 transitions, while the remaining transitions are nonstretched dipoles. It is clear from the results that the SA resolution improves when the preponderance of E2 transitions is decreased, i.e. that of the nonstretched dipoles is increased.

Realistic cascades from heavy-ion induced fusion reactions involve mainly stretched E2 transitions with smaller numbers of stretched and unstretched dipoles. Such responses are illustrated in fig. 8 for a fixed value of $M_\gamma = 25$ and for the (M_{22}, M_{11}, M_{10}) combinations: (a) (25, 0, 0), (b) (19, 3, 3) and (c) (17, 4, 4), respectively. It is clearly seen that as the total number of dipoles increases at the expense of stretched E2 transitions, the SA resolution does not deteriorate significantly as long as the number of stretched and nonstretched dipole transitions remains equal. This is the main reason for the wide applicability of the SA technique in nuclei that are not necessarily very good rotors, although the ratio of stretched to nonstretched dipole transitions in the cascade can deviate to a large extent from unity.

4.2. Perturbations in the SA distributions from uneven efficiencies

The effect of uneven efficiencies of the NaI detectors in the spin spectrometer on the SA distributions is best

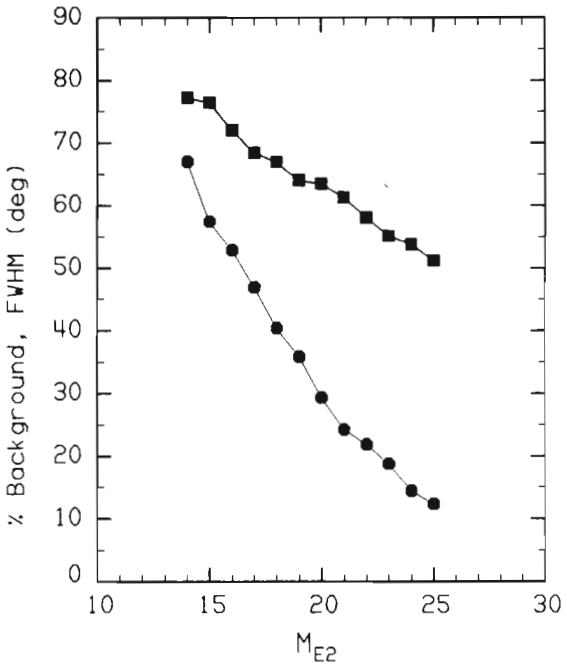

Fig. 6. Plots of the Gaussian width (solid squares) and of the constant background percentage (solid circles) fitted to the SA responses as a function of the number of stretched E2 transitions. The remaining transitions from a total of 25 are all stretched dipole transitions. Only the cascades for which the distribution had its peak at the correct spin direction were included in this figure. The lines are for guiding the eye.

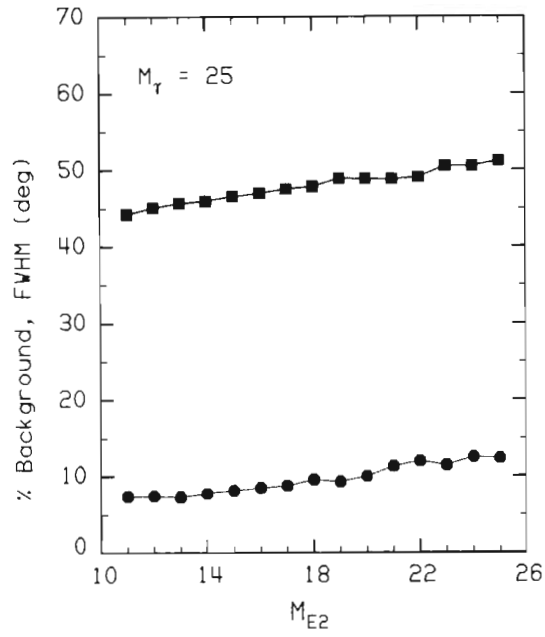

Fig. 7. Width of Gaussian (solid squares) and the associated background fraction (solid circles) of fitted SA responses from cascades of total $M_\gamma = 25$ as a function of the number of stretched quadrupoles M_{E2}, while the remaining transitions are nonstretched ($\Delta I = 0$) dipoles. It is seen that as M_{E2} decreases the SA resolution improves.

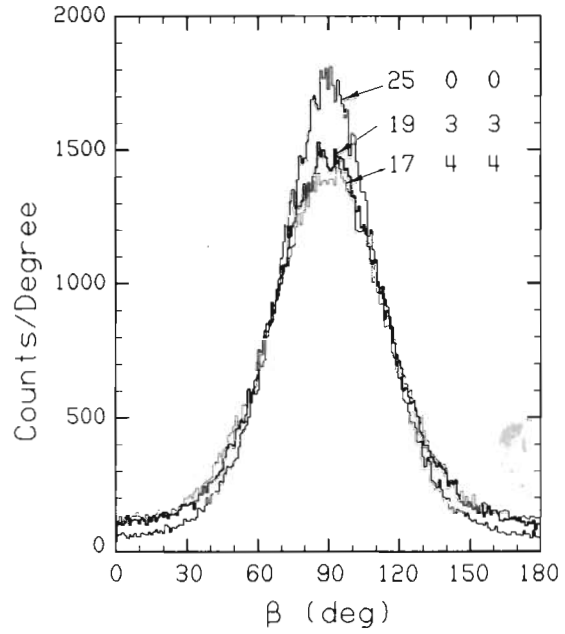

Fig. 8. Comparison of the SA responses for three different incoherent multipole admixtures. The multiplicities M_{E2}, $M_{E1(\Delta I=-1)}$, $M_{E1(\Delta I=0)}$ cited are for stretched quadrupoles, stretched dipoles, and nonstretched dipoles, respectively. The SA resolution does not deteriorate significantly when both types of stretched and non-stretched dipoles are present. This is due to their mutual effect.

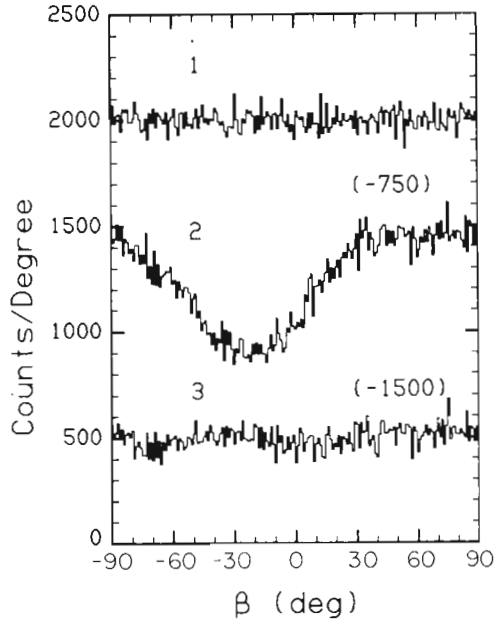

Fig. 9. Curve 1 shows the measured spin distribution obtained by sorting simulated events generated with a uniform initial spin distribution, and a uniform detector efficiency in the spectrometer. Curve 2 shows the distribution obtained from events created with a uniform initial distribution but with one detector at $\theta = 93°$ and $\phi = 67°$ removed from the spectrometer. Curve 3 shows the distribution from the data of curve 2 after correction for the hole during sorting, using the local density method described in the text.

understood if we examine their influence on (a) an equally populated (flat) distribution of spin orientations, (b) the position of the estimated spin direction, and (c) the SA resolution.

First, events with uniform distribution of spin orientations for equal efficiency of the detectors in the spectrometer are created. When these events are sorted with the SA searching routine a uniform distribution of spin orientations shown by curve 1 in fig. 9 is obtained. Next events from an initially uniform distribution of spin orientations are created with a hole introduced in the spectrometer by removing the detector located at $\theta = 93°$ and $\phi = 67°$. The new events are then sorted without any correction and the distribution shown by curve 2 in fig. 9 is obtained. This distribution exhibits a 24% dip at $-23°$ and clearly shows that the routine preferably finds the spin direction shifted towards the hole in the spectrometer. After the correction routine for the existence of the hole is applied, using the local-density distributions to compensate for the missing detector, then the distribution shown by curve 3 in fig. 9 is obtained. This curve shows that only a small ($\pm 1.5\%$) modulation remains on the corrected perturbed distribution. The magnitude of the perturbation depends on the polar angle θ of the removed detector and has its maximum at $\theta = 90°$. The dependence of the perturbation (dip) on the polar angles (θ, ϕ) is shown in fig. 10. When the angle θ is kept near 90° and ϕ of the removed detector is varied, the dip tracks exactly the angle $\phi - 90°$ as shown in fig. 10a. On the other hand, when ϕ is kept approximately at 90° and θ of the hole is varied, the position of the dip stays at approximately 0° but its magnitude increases for θ going from 24.4° to 77.5°, as it is shown in fig. 10b. The explanation for the appearance of the dip at 90° to the hole is the following. The absence of the counts in the position of the hole has an effect on the search routine which is analogous to the position of the "hole of the doughnut". Therefore, the routine finds with higher probability the spin direction to be in the direction of the hole, which means it produces a bump at the hole position and a dip at 90° to it.

The perturbation on the derived spin distribution due to the presence of more than one hole in the spectrometer has a cumulative effect. This is indeed observed in fig. 11a in which curves labelled 1 through 4 correspond to 1 to 4 detectors removed from the spectrometer at the indicated (θ, ϕ) positions. A dip down to 38% of the maximum is observed when 4 detectors are removed. The data for fig. 11 have been created with 5000 events/deg. in the original spin distribution. It is quite clear that since number of events is conserved, the missing intensity from the dip in fig. 11a appears at other angles. The corrected distributions using the local-density method are shown in fig. 11b. For the most perturbed case (curve 4) the peak-to-valley

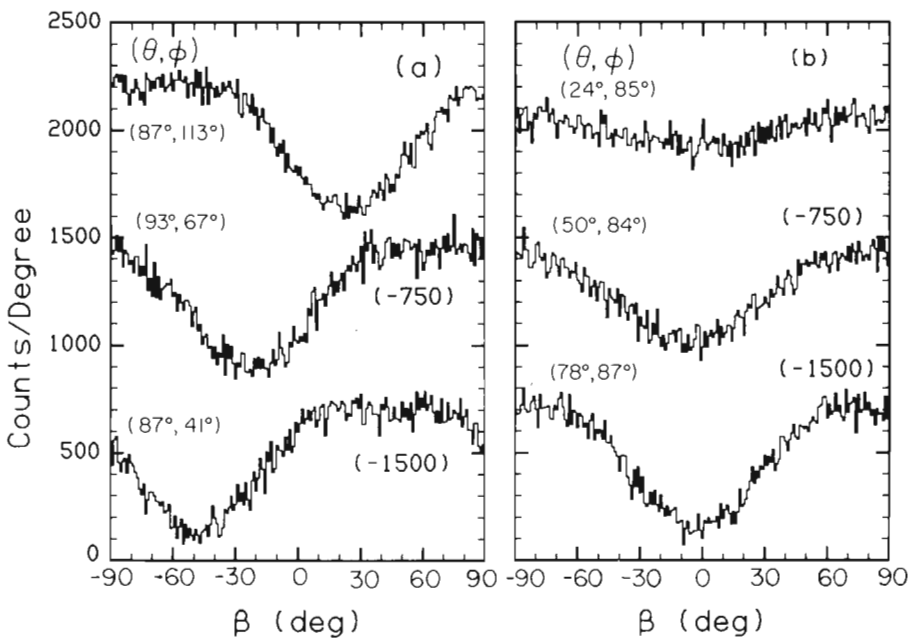

Fig. 10. Part (a) shows the shift in the position of the dip in the deduced spin distribution as the azimuthal angle ϕ of the hole in the spectrometer is varied from 41° to 113° (the polar angle θ is kept within the range $90° \pm 3°$). Part (b) shows the increase in magnitude of the dip as the polar angle is increased from 24° to 78°, while the azimuthal angle ϕ is kept near 90°.

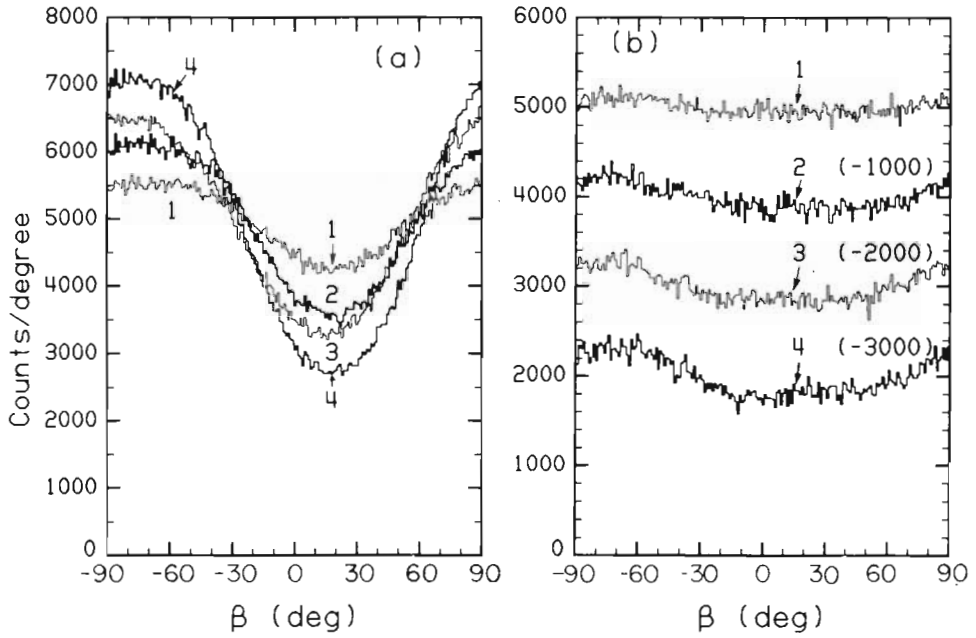

Fig. 11. In part (a) Curve 1 shows the derived spin distribution from an initially uniform population when a detector at (θ, ϕ) of (63°, 108°) was removed. Curve 2 shows the derived distribution when an additional detector at (116°, −72°) is removed. For curve 3 the detector at (42°, −94°) was also removed, and for curve 4 the fourth detector at (112°, 118°) was also removed. The effect of the additional holes is seen to be cumulative, enhancing the magnitude of the dip. In part (b) curves 1 through 4 correspond to those in part (a) when the data were sorted by the routine applying the correction for the presence of the holes, based on the local hit-density method.

ratio is reduced from 2.58 : 1 to 1.09 : 1 when the correction is applied, while for the case of smallest perturbation (curve 1) it is reduced from 1.29 : 1 to 1.03 : 1. It should be emphasized that the θ-position of a hole (or a low-efficiency detector) has the same significance as that of a triggering detector, like an α detector, which is used to measure the angular distribution of the particles it measures (e.g. α particles) with respect to the spin direction. When the hole is at $\theta = 90°$ it covers the whole 0°–90° angular range with respect to the spin direction, but when it is close to 0° it is almost always at 90° to the spin direction, and therefore the perturbation it introduces is small. By the same token α detectors positioned at $\theta = 90°$ can measure all the possible α spin angles, but the ones positioned close to $\theta = 0°$ measure only a small angular range.

A less pronounced effect of the presence of holes or uneven efficiencies is expected on the position and the width of the derived distribution of spin orientations when the initial spins are at a fixed angle. To demonstrate this, events were generated with fixed initial spin direction at 90°. Holes were created at a variety of ϕ angles that differed from 90° by 24° to 167°, while the θ values were chosen to be as close to 90° as possible. These event sets were then sorted with and without corrections for the missing detector. The results are summarized in table 1. It is seen that the presence of a hole on one side of the initial spin direction attracts the estimated spin direction to that side. The shifts in angle can be as large as 5°. The widths can vary by

Table 1
Shifts in spin alignment position and its distribution width due to introduction of holes at the indicated angles with respect to the initial spin direction. The initial spins were at $\beta = 90°$. The events are made of 25 γ transitions, all stretched E2.

ϕ_{hole} (deg)	Uncorrected events Deduced		Corrected events Deduced	
	$\langle\beta\rangle$ [a]	fwhm(%)	$\langle\beta\rangle$ [a]	fwhm(%)
(no hole)	90.4	57.6	–	–
+66°	85.6	59.9	89.2	59.7
+114°	94.9	58.0	91.3	56.9
+41°	86.2	56.0	90.0	59.4
+139°	94.6	55.4	90.6	58.5
−5°	89.9	57.3	90.5	58.2
+185°	91.0	57.3	90.4	57.3
−31°	87.3	54.7	90.2	57.8
+211°	93.5	55.8	90.6	58.8
−77°	87.9	62.6	90.2	57.2
+257°	93.4	63.6	90.9	59.0

[a] $\langle\beta\rangle$ in degrees.

$\pm 8\%$ from the unperturbed values. These perturbations decrease as the angle θ of the hole departs from 90°.

5. Angular distributions of α particles with respect to the spin direction

An interesting application of the spin alignment technique for determining the spin direction on an event-by-event basis is in measurement of the angular distribution of α particles with respect to the spin direction in fusion reactions. For this purpose an α-detector, i.e. a $(\Delta E, E)$ Si telescope can be used. As mentioned before, it should be located at an angle $\theta_{CM} = 90°$ with respect to the beam direction in the center of mass system in order to measure yield of the α particles over the whole angular range of 0°–90° with respect to the spin direction. Fig. 12 shows such an angular distribution measured for 21 MeV α particles produced in the reaction of 175 MeV ^{20}Ne with ^{150}Nd. The α particles were detected at 90° in the center of mass, for a gamma fold k_γ between 23 and 26 [4]. The angle β with respect to the estimated spin direction was sampled at 18° bins in order to increase statistics for each bin. In order to extract the corrected angular distribution with respect to the spin direction, the SA response of the spin spectrometer for parameters relevant to the reaction was produced. Simulated response for the appropriate γ ray multiplicity and multipole mixing were derived from an angular distribution analysis of the γ rays with respect to the beam direction. Other factors that attenuate or flatten the SA response and were included in the simulated responses were (a) the quantum mechanical tilting which is given by $\cos\beta' = \sqrt{I/(I+1)}$, (b) the finite aperture size of the α detector and the uncertainty in measurement of the emission direction of the α particle, and (c) the loss in alignment due to nonstretched particle emission. After these effects were incorporated in the SA response, a Legendre polynomial expansion of the type $A_0[1 + A_2P_2(\cos\beta) + A_4P_4(\cos\beta)]$ was found which upon convolution with the response function reproduced the experimental angular distribution with respect to the spin direction.

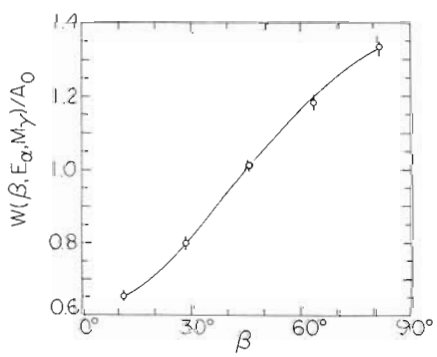

Fig. 12. Angular distribution of α particles with respect to the estimated spin direction. The α particles were detected at $\theta_{CM} = 90°$ with respect to the beam from the reaction of 175 MeV ^{20}Ne on ^{150}Nd. The curve is a least squares fit to the function $A_0[1 + A_2P_2(\cos\beta) + A_4P_4(\cos\beta)]$ (from ref. [4]).

6. Conclusions

It is demonstrated that for fusion reactions populating high spin states which decay with a preponderance of γ transitions with a specific direction of emission with respect to the spin direction of the evaporation residues, it is possible to derive the spin direction on an event-by-event basis using a device like the spin spectrometer. The detailed dependence of the SA response on γ ray multiplicity and multipolarity has been outlined. Extreme caution must be exercised for the cases that the cylindrical symmetry of the efficiency of the spin spectrometer is broken, as in the case that NaI detectors are removed from the spin spectrometer, since erroneous angular distributions may result. In such cases correction for detection nonuniformity is essential. A method based on the local density distribution was offered and its applicability and success were discussed in detail. A specific example of an angular distribution of α particles with respect to the estimated spin direction was also presented.

Acknowledgements

This work was supported in part by the US Department of Energy under contract No. DE-AS02-76ER 04052. Oak Ridge National Laboratory is operated by Martin Marietta Energy Systems, Inc., under contract No. DE-AC05-840R21400 with the US Department of Energy.

References

[1] R.M. Diamond and F.S. Stephens, Ann. Rev. Nucl. Part. Sci. 30 (1980) 85.
[2] M. Jääskeläinen, D.G. Sarantites, R. Woodward, F.A. Dilmanian, H. Puchta, J.R. Beene, J. Hattula, M.L. Halbert, D.C. Hensley and J.H. Barker, Phys. Rev. Lett. 49 (1982) 1387.
[3] M. Jääskeläinen, D.G. Sarantites, F.A. Dilmanian, R. Woodward, H. Puchta, J.R. Beene, J. Hattula, M.L. Halbert and D.C. Hensley, Phys. Lett. 119B (1982) 65.
[4] F.A. Dilmanian, D.G. Sarantites, M. Jääskeläinen, H. Puchta, R. Woodward, J.R. Beene, D.C. Hensley, M.L. Halbert, R. Novotny, L. Adler, R.K. Choudhury, M.N.

Namboodiri, R.P. Schmitt and J.B. Natowitz, Phys. Rev. Lett. 49 (1982) 1909.
[5] D.G. Sarantites, R. Lovett and R. Woodward, Nucl. Instr. and Meth. 171 (1980) 503.
[6] M. Jääskeläinen, D.G. Sarantites, R. Woodward, F.A. Dilmanian, J.T. Hood, R. Jääskeläinen, D.C. Hensley, M.L. Halbert and J.H. Barker, Nucl. Instr. and Meth. 204 (1983) 385.
[7] D.G. Sarantites, M. Jääskeläinen, R. Woodward, F.A. Dilmanian, D.C. Hensley, J.H. Barker, J.R. Beene, M.L. Halbert and W.T. Milner, Phys. Lett. 115B (1982) 441.
[8] J.M. Blatt and V.F. Weisskopf, Theoretical Nuclear Physics (Wiley, New York, 1952) p. 594.
[9] L. Westerberg, D.G. Sarantites, K. Geoffroy, R.A. Dayras, J.R. Beene, M.L. Halbert, D.C. Hensley and J.H. Barker, Phys. Rev. Lett. 41 (1978) 96.
[10] D.F. Morrison, Multivariate Statistical Methods (McGraw-Hill, New York, 1967), p. 82.
[11] M. Gyulassy et al. Phys. Lett. 110B (1982) 185.
[12] A. Holm, IEEE Trans. Nucl. Sci. NS-30 (1983) 3983.